Magnetoelectric phase control in a magnetic system showing cycloidal/conical spin order

2008 J. Phys.: Condens. Matter 20 434204

(http://iopscience.iop.org/0953-8984/20/43/434204)

IOP PUBLISHING JOURNAL OF PHYSICS: CONDENSED MATTER

J. Phys.: Condens. Matter **20** (2008) 434204 (8pp) doi:10.1088/0953-8984/20/43/434204

Magnetoelectric phase control in a magnetic system showing cycloidal/conical spin order

T Kimura[1] **and Y Tokura**[2,3,4]

[1] Division of Materials Physics, Graduate School of Engineering Science, Osaka University, 1-3 Machikaneyama, Toyonaka, Osaka 560-8531, Japan
[2] Department of Applied Physics, University of Tokyo, 7-3-1 Hongo, Bunkyo-ku, Tokyo 113-8656, Japan
[3] Multiferroics Project, ERATO, JST, c/o University of Tokyo, Tokyo 113-8656, Japan
[4] Cross-Correlation Materials Research Group, FRS, RIKEN, Wako 351-0198, Japan

E-mail: kimura@mp.es.osaka-u.ac.jp and tokura@ap.t.u-tokyo.ac.jp

Received 4 March 2008, in final form 8 May 2008
Published 9 October 2008
Online at stacks.iop.org/JPhysCM/20/434204

Abstract

Since the discovery of ferroelectric activity as well as colossal magnetoelectric response in a perovskite-type manganite $TbMnO_3$, the study of a new class of magnetoelectric multiferroics has been attracting a great deal of interest. In these multiferroics, ferroelectric order develops upon a magnetic phase transition into some *spiral* magnetic ordered phases such as a *cycloidal* or *transverse conical* structure. Since the origin of ferroelectricity is attributed to magnetism in these multiferroics, ferroelectric properties can be readily controlled by the use of magnetic fields. We review the magnetoelectric phase control in a magnetic system showing cycloidal/conical spiral spin order.

(Some figures in this article are in colour only in the electronic version)

1. Introduction

The study of magnetoelectric multiferroics [1, 2] in which both magnetic and ferroelectric orders coexist attracted considerable interest in the 1960s and 1970s [3]. In magnetoelectric multiferroics, one can realize complex phenomena such as the magnetoelectric (ME) effect, i.e. the generation of electric polarization by a magnetic field or magnetization by an electric field [4, 5]. However, in most of the early multiferroics, the temperature scale for ferroelectric order is much larger than for magnetic order. In other words, the origins of these orders have no relation to each other. This leads to only weak coupling between magnetism and ferroelectricity in these systems. About five years ago, ferroelectric order accompanied by a magnetic phase transition has been found for perovskite-type rare-earth manganites, $TbMnO_3$ and $DyMnO_3$, which show antiferromagnetic orders with long wavelengths and remarkable ME effects driven by metamagnetic transitions [6, 7]. The discovery of the spin-driven ferroelectricity triggered rapid developments in the exploration of new multiferroics (e.g. $Ni_3V_2O_8$ [8] and $CoCr_2O_4$ [9]) and motivated an extensive study to understand the origin of ferroelectricity in known multiferroics such as RMn_2O_5 (R = rare-earth or Bi) [10, 11]. A characteristic property of these multiferroics is the simultaneous occurrence of a ferroelectric phase transition and a *noncollinear spiral* magnetic order. Thus, the spiral magnetism is the key to understanding the ferroelectric and magnetoelectric properties in these multiferroics. Because spiral magnetic order often arises from the competition between nearest-neighbor and further-neighbor magnetic interactions, systems containing competing magnetic interactions (spin frustration) are promising candidates for this class of multiferroics. On the basis of this strategy several new multiferroics related to spiral magnetic orders have been found in the past few years. This means the emergence of a new class of ferroelectrics in which the origin of ferroelectricity is driven by spiral magnetism and is completely different from that in conventional ferroelectrics.

There are several types of spiral magnetic structures. The classification of the spiral type is critical for understanding the

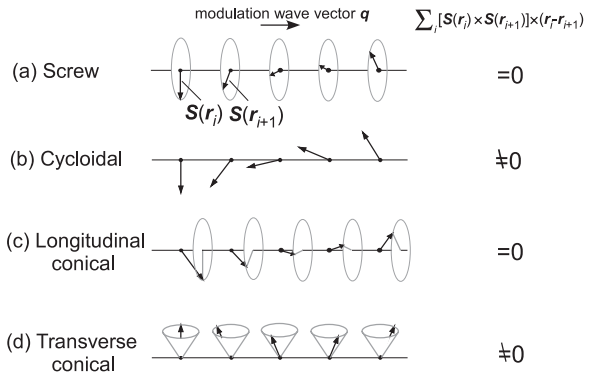

Figure 1. Schematic illustrations of types of spiral magnetic structures on a one-dimensional array of magnetic moments $\boldsymbol{S}(\boldsymbol{r})$. (a) Screw, (b) cycloidal, (c) longitudinal conical and (d) transverse conical. The magnitudes of $\sum_i [\boldsymbol{S}(\boldsymbol{r}_i) \times \boldsymbol{S}(\boldsymbol{r}_{i+1})] \times (\boldsymbol{r}_i - \boldsymbol{r}_{i+1})$ are also listed for their respective structures.

spiral-spin-driven ferroelectricity. In figure 1, we schematically depict various noncollinear spiral magnetic structures on a one-dimensional array of magnetic moments $\boldsymbol{S}(\boldsymbol{r})$. Here, the direction of $(\boldsymbol{r}_{i+1} - \boldsymbol{r}_i)$ is along the magnetic modulation wavevector $\boldsymbol{q}$ of the spiral structure, and $[\boldsymbol{S}(\boldsymbol{r}_i) \times \boldsymbol{S}(\boldsymbol{r}_{i+1})]$ gives the spin rotation axis. If the spin rotation axis is parallel to the modulation wavevector, the arrangement gives a *screw* spiral structure (figure 1(a)). If the spin rotation axis is perpendicular to the propagation vector of the spiral, the resulting arrangement is termed a *cycloidal* spiral structure (figure 1(b)). A rather more complicated system is a *conical* spiral in which a ferromagnetic component coexists with a screw or cycloidal component for longitudinal (figure 1(c)) or transverse (figure 1(d)) conical structure, respectively. These conical structures are generally obtained by applying weak magnetic fields to screw or cycloidal spiral structures. However, in some compounds such as $CoCr_2O_4$, the conical structure can be stabilized even at zero magnetic field, which is also discussed in this paper.

In this paper, we review the particular class of magnetoelectric multiferroics in which noncollinear spiral magnetism realizes complex control of magnetic and electric properties by using either a magnetic field H or electric field E.

2. Magnetic field control of polarization in perovskite $RMnO_3$

First, we show the ferroelectric property which is coupled with the magnetic one in perovskite-type rare-earth manganites $RMnO_3$ (R = Tb and Dy) as a typical example of spiral-spin-driven ferroelectrics [6, 7, 12]. The fundamental crystal structure of these manganites is the *Pbnm* orthorhombic nonpolar structure, as illustrated in the inset of figure 2. Upon cooling, the system shows successive magnetic phase transitions. Figure 2 shows temperature profiles of specific heat divided by temperature (upper panels) and electric polarization P along the c axis (lower panels) of $TbMnO_3$ (left) and $DyMnO_3$ (right). The anomaly in specific heat at T_N (41 K for $TbMnO_3$ and 39 K for $DyMnO_3$) corresponds to an antiferromagnetic ordering with a modulation wavevector (0, k, 1) [13, 14]. The k (∼0.29 for $TbMnO_3$) is incommensurate at T_N and decreases with decreasing temperature. The second anomaly is observed in specific heat at T_C (28 K for $TbMnO_3$ and 19 K for $DyMnO_3$). In these manganites, ferroelectric order with spontaneous polarization along the c axis develops below T_C, as shown in the lower panels of figure 2. Below T_C, the k (∼0.28 for $TbMnO_3$) shows little temperature dependence. Upon further decreasing temperature, the temperature dependence of the specific heat shows the third

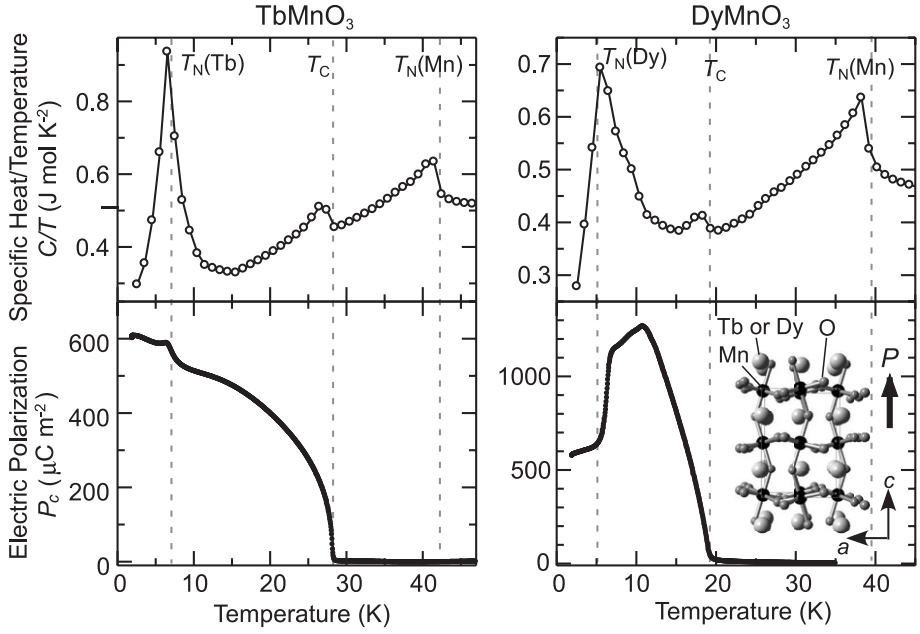

Figure 2. Magnetic and ferroelectric phase transitions in multiferroic perovskite-type rare-earth manganites. Temperature profiles of (upper panels) specific heat divided by temperature and (lower panels) electric polarization along the c axis in (left panels) $TbMnO_3$ and (right panels) $DyMnO_3$. The inset shows the fundamental crystal structure of the rare-earth manganites and the direction of electric polarization P.

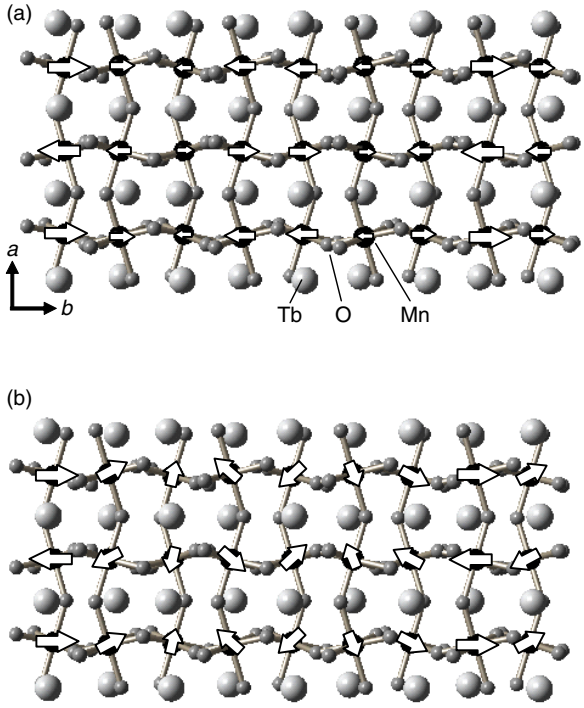

Figure 3. Rough sketches of proposed magnetic structures at Mn sites in (a) paraelectric antiferromagnetic phase ($T_C \leqslant T \leqslant T_N$) and (b) ferroelectric antiferromagnetic phase ($T \leqslant T_C$) of $TbMnO_3$ [15].

anomaly at ∼7 K and ∼5 K where the Tb^{3+} and Dy^{3+} moments undergo long-range ordering, respectively. Around this temperature, the electric polarization also exhibits a distinct anomaly. These results indicate that ferroelectricity in these manganites strongly couples with the magnetic property.

A sinusoidally modulated collinear magnetic structure model (figure 3(a)) was formerly proposed by an early neutron diffraction study of $TbMnO_3$ at all temperatures below T_N [13]. However, a recent neutron diffraction measurement by Kenzelmann and coworkers [15] proposed a different magnetic structure model for the ferroelectric phase below T_C. Their proposed model below T_C is an elliptically modulated *cycloidal* spiral magnetic structure which is illustrated in figure 3(b). This spin structure has also been confirmed in a similar rare-earth manganite endowed with ferroelectricity, $Tb_{1-x}Dy_xMnO_3$, where the *commensurate* propagation wavevector ($k = 1/3$) is observed in the ferroelectric state by a model-free analysis using single-crystal neutron diffraction data [16]. These results clearly demonstrated that the magnetic structure is *collinear* in the paraelectric antiferromagnetic phase while that in the ferroelectric phase shows a *noncollinear cycloidal spiral* spin structure. This appearance of the cycloidal spiral spin structure accompanied by a ferroelectric phase transition is important in understanding the origin of ferroelectricity in these multiferroic manganites.

Magnetic control of the ferroelectric property in the rare-earth manganite can be seen in the P–E curves measured at applied magnetic fields. In figure 4, we show the 15 K P–E curves obtained at 0 and 4 T for $DyMnO_3$. Here, magnetic

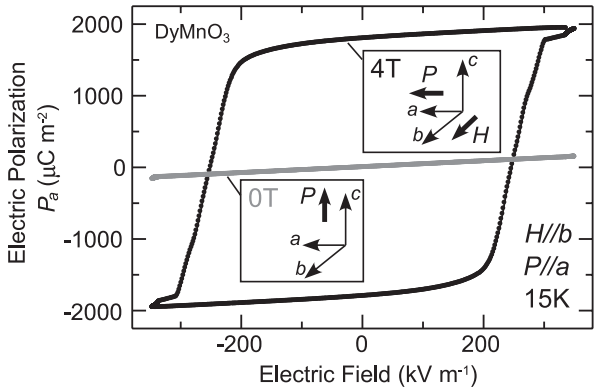

Figure 4. Magnetic control of ferroelectric property. P–E curves obtained at magnetic fields of 0 T (gray) and 4 T (black) at 15 K for $DyMnO_3$. Magnetic and electric fields are applied along the b and a axes, respectively. Schematic drawings in the insets show the relationships among crystallographic axes, magnetic field and electric polarization.

fields were applied along the b axis while electric fields were parallel to the a axis. Since $DyMnO_3$ shows spontaneous polarization along the c axis in the absence of magnetic fields, no hysteresis loop is observed in P along the a axis at 0 T (a gray line in figure 4). By contrast, a clear hysteresis loop characteristic of ferroelectrics is seen in a magnetic field of 4 T (a solid line). This remarkable magnetic control of the ferroelectric property is observed in the ferroelectric state with the ferroelectric polarization direction switched from the c to the a axis by applying magnetic fields along the b axis, as illustrated in the insets of figure 4. The hysteretic reversal of P with E means the switch of the spin helicity (vector spin chirality) in the ab-plane spiral, as elucidated in the next section.

3. Cycloidal spin ferroelectrics

A cycloidal spiral magnetic structure accompanied by ferroelectric order shown in the previous section is a key to the understanding of the ferroelectricity in $RMnO_3$ (R = Tb and Dy). A microscopic mechanism of the spiral-spin-driven ferroelectricity has been proposed by Katsura and coworkers [17]. They consider that spin current (or vector spin chirality), $\boldsymbol{S}(\boldsymbol{r}_i) \times \boldsymbol{S}(\boldsymbol{r}_{i+1})$, induced between noncollinearly-coupled spins at an angle ($\neq 0, \pi$) leads to local electric polarization which is given by the following equation:

$$\boldsymbol{P} = \gamma[\boldsymbol{S}(\boldsymbol{r}_i) \times \boldsymbol{S}(\boldsymbol{r}_{i+1})] \times (\boldsymbol{r}_i - \boldsymbol{r}_{i+1}). \qquad (1)$$

Here γ is a constant related to the spin–orbit coupling and superexchange interactions. This can be regarded as an inverse effect of the antisymmetric Dzyaloshinskii–Moriya (DM) interaction where two noncollinearly coupled magnetic moments displace the oxygen intervening between them through the electron–lattice interaction [18]. Equation (1) indicates that a finite electric polarization can appear when adjacent magnetic moments are coupled noncollinearly in a spiral manner and the spin rotation axis is not parallel to the

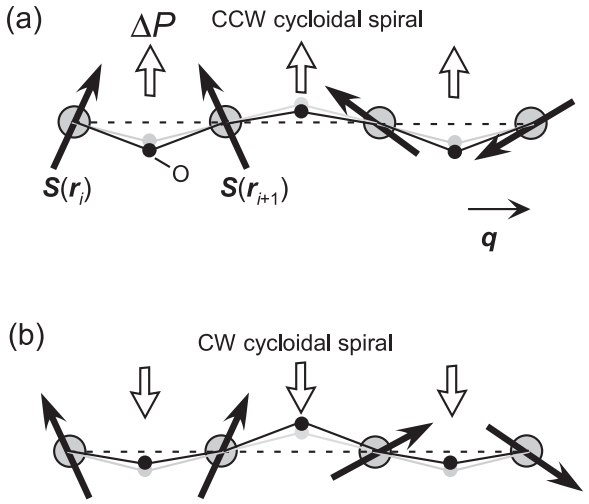

Figure 5. Two domains ((a) counterclockwise and (b) clockwise) of a cycloidal spiral structure. These two domain structures are converted into each other by space inversion. Here $\boldsymbol{q}$ is the propagation vector of the magnetic structures. The difference between the gray and black circles corresponds to the shift of the oxygen ions due to the inverse DM effect. The white arrows denote the resultant change of the local electric polarization ΔP.

propagation vector (i.e. cycloidal structure). A schematic drawing of the configuration is shown in figure 5(a). When the magnetic moments are aligned in a cycloidal spiral manner, the direction of the local electric polarization induced by the inverse DM interaction is uniform in the system and the macroscopic electric polarization can emerge. Since the exchange of two moments reverses the sign of the effect in the asymmetric DM interaction, the direction of the induced electric polarization can be reversed by reversal of spin helicity (figure 5(b)). Phenomenological treatments using Landau theory have also been reported by Harris *et al* [8, 15] and Mostovy [19]. These recent theoretical studies deduced the general relation between the electric polarization and the magnetic moments in the system with spiral magnetic structures from symmetry considerations.

In the inverse DM scenario or the spin-current model, not only a cycloidal spiral (figure 1(b)) but also a transverse conical (figure 1(c)) spiral in which $\sum_i [\boldsymbol{S}(\boldsymbol{r}_i) \times \boldsymbol{S}(\boldsymbol{r}_{i+1})] \times (\boldsymbol{r}_i - \boldsymbol{r}_{i+1}) \neq 0$ meet the requirements for the appearance of finite electric polarization. In contrast, a screw spiral (figure 1(a)) and a longitudinal cycloidal (figure 1(c)) structure with $\sum_i [\boldsymbol{S}(\boldsymbol{r}_i) \times \boldsymbol{S}(\boldsymbol{r}_{i+1})] \times (\boldsymbol{r}_i - \boldsymbol{r}_{i+1}) = 0$ cannot induce a net polarization, except for specific lattice forms (see below). In fact, this spin-current model or the inverse DM scenario well explains the ferroelectricity of cycloidal $RMnO_3$ (R = Tb and Dy) in which P appears in the direction along the c axis, i.e. perpendicular to both the spin rotation axis ($\parallel a$ axis) and the propagation vector of the spiral ($\parallel b$ axis). Furthermore, a recent polarized neutron diffraction measurement confirmed that spin helicity can be reversed by sign reversal of poling electric fields in the ferroelectric phase of $TbMnO_3$ [20].

The theoretical studies described above indicate that spiral magnets are endowed with a multiferroic nature as well as a large magnetoelectric effect, and hence that magnetoelectric multiferroics should be seen in a much wider range of compounds. Based on this strategy, in the past several years, ferroelectricity and/or large magnetoelectric effect have been found in several cycloidal spiral systems such as $Ni_3V_2O_8$ [8], $CoCr_2O_4$ [9], $MnWO_4$ [21], $LiCu_2O_2$ [22], $LiCuVO_4$ [23] and CuO [24]. In the case of $CoCr_2O_4$, ferroelectric order is accompanied by a *conical* spiral order [9]. The magnetic structure of $CoCr_2O_4$ corresponds to the *transverse* conical structure illustrated in figure 1(c). Since a cycloidal component coexists with a ferromagnetic component in the transverse conical structure, ferroelectricity of $CoCr_2O_4$ can also be categorized into cycloidal spiral origin. This compound is unique among compounds in having spontaneous magnetization due to the ferromagnetic component, as detailed in the next section.

Apart from cycloidal/transverse conical structures, some screw spiral magnets such as $CuFeO_2$ [25] also host the spontaneous electric polarization. The appearance of finite electric polarization in screw spiral systems cannot be explained by the spin-current model and the inverse DM model. Recently, Arima proposed the possibility of ferroelectricity in monoclinic (or rhombohedral) crystals with a proper screw spiral magnetic order in which the spin rotation axis is parallel to the propagation vector of the spiral [26]. He pointed out that in a monoclinic system the removal of the (glide) mirror symmetry by a proper screw magnetic structure produces a polar system with polarization. This indicates that any spiral spin structure can induce finite electric polarization on the low-symmetry lattices.

4. Transverse conical spin ferroelectrics

In figure 1, we showed the general spiral spin structures which can potentially host the magnetoelectric effect and/or spin-driven ferroelectricity. As far as the inverse DM model [18] or the spin-current model [17], as expressed by equation (1), is concerned, the transverse-spiral spin structure can produce the ferroelectricity. $RMnO_3$, as described in the earlier sections, is typical of magnetic ferroelectrics based on this mechanism, while showing no spontaneous magnetization. The present scenario can be extended to the transverse conical spin state (figure 1(d)) in which the spontaneous (homogeneous) and spiral components of the magnetization can coexist. This may lead to the real (i.e. both ferromagnetic and ferroelectric) multiferroics of magnetic origin. Here we present the two prototypical cases; Cr-based spinel compounds of $CoCr_2O_4$ [9] and $ZnCr_2Se_4$ [27]. The former is a generic conical magnet, while the latter is an originally proper screw helimagnet (figure 1(a)) but turned into a conical state under the magnetic field applied along the slanted direction off the screw axis.

In $CoCr_2O_4$ (figure 6), the magnetic Co^{2+} ions occupy the A (8a) sites and the Cr^{3+} ions the B (16d) sites in the normal spinel structure. The ferrimagnetic transition occurs at $T_C = 93$ K, and with further lowering the temperature the compound undergoes the transition to the conical spin states, i.e. the ferromagnetic plus transverse-spiral spin state, with the incommensurate propagation vector of $[qq0]$ ($q \sim 0.63$) at $T_S = 26$ K [27–30]. The incommensurate–commensurate

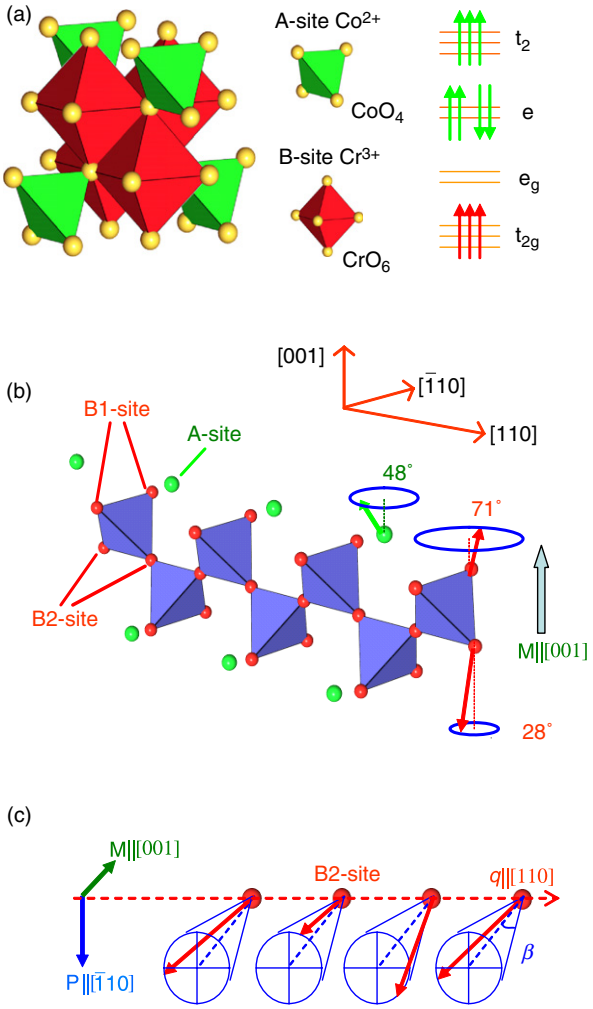

Figure 6. Schematic structure of spinel $CoCr_2O_4$ and the electronic configurations of constituent Co^{2+} and Cr^{3+} ions. (b) The structure viewed along the conical spin modulation direction [110] (denoted as the x axis). The circles with slanted arrows indicate the spiral plane of the respective spins with conical structure. (c) The relation among the net magnetization M, the spiral spin modulation vector $\boldsymbol{q}$ and the induced polarization P, as represented for the case of the B_2-site chain in $CoCr_2O_4$.

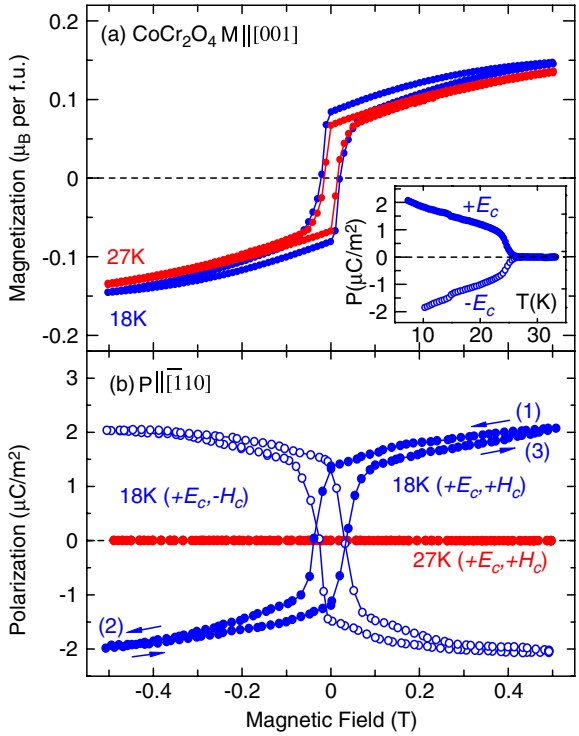

Figure 7. Magnetic field dependence of (a) magnetization and (b) electric polarization at temperatures above (27 K) and below (18 K) the ferroelectric transition temperature ($T_s = 26$ K). For measurement of the polarization (b), the magnetic field was scanned between $+H_c$ and $-H_c$, for each ME-cooled state prepared with (E_c, H_c) and (E_c, $-H_c$), as represented by closed and open circles. E_c (=400 kV m^{-1}) and H_c (=0.5 T) stand for the cooling electric and magnetic fields, respectively. The inset to (a) shows the temperature dependence of spontaneous polarization in the cases of the ME cooling with positive and negative E_c. Cited from [9].

or lock-in transition occurs around 15 K without changing much the q value [31]. As shown in figure 6, the spiral plane in which the rotating spin moments lie is the (001) plane, while the spontaneous magnetization is directed along the [001] or equivalent directions. Then, according to the above spin-current model, the spontaneous polarization vector is expected to lie within the (001) spiral plane and perpendicular to the [110] propagation vector, and therefore along the [1$\bar{1}$0] axis perpendicular to the [001] spontaneous magnetization direction.

The inset to figure 7 shows the temperature dependence of polarization, which was deduced from the pyroelectric current in the zero electric and magnetic field warming after the magnetoelectric (ME) cooling procedure [9]. The polarization P shows the onset at T_S (=26 K) and subsequently a tiny anomaly at T_{C-IC} (=15 K). The direction of the spontaneous polarization was confirmed to coincide with that of the electric field E_c applied in the ME cooling procedure, as shown in the inset to figure 7. Thus, the observed P is the spontaneous polarization in the ferroelectric phase below T_S, irrespective of the spin spiral state being commensurate or incommensurate.

We show in figure 7(b) the magnetic field dependence of the polarization at selected temperatures (18 and 27 K) in comparison with the conventional magnetization curve (figure 8(a)). Prior to the magnetic field scan, the polarization direction could be completely determined by the direction of the cooling electric field (E_c = 400 kV m^{-1}) in the aforementioned ME cooling procedure, as shown in the inset. Then the magnetic field (H_c = 0.5 T) was scanned between $+H_c$ and $-H_c$. As clearly seen in figure 7(b), whichever direction of the magnetization is taken as the starting point, the polarization is always reversed upon the reversal of the magnetization direction (figure 7(a)).

The synchronized reversal of the spontaneous polarization and magnetization can be more directly confirmed by the sequential scan of the magnetic field between +0.2 and −0.2 T at 18 K, as shown in figure 8 [9]. The magnitude of flopped P is almost constant and reaches the full value as observed by the quasi-static measurement (see the inset to figure 7). The ferroelectric and ferromagnetic single-domain feature, which was achieved by the ME cooling procedure, was

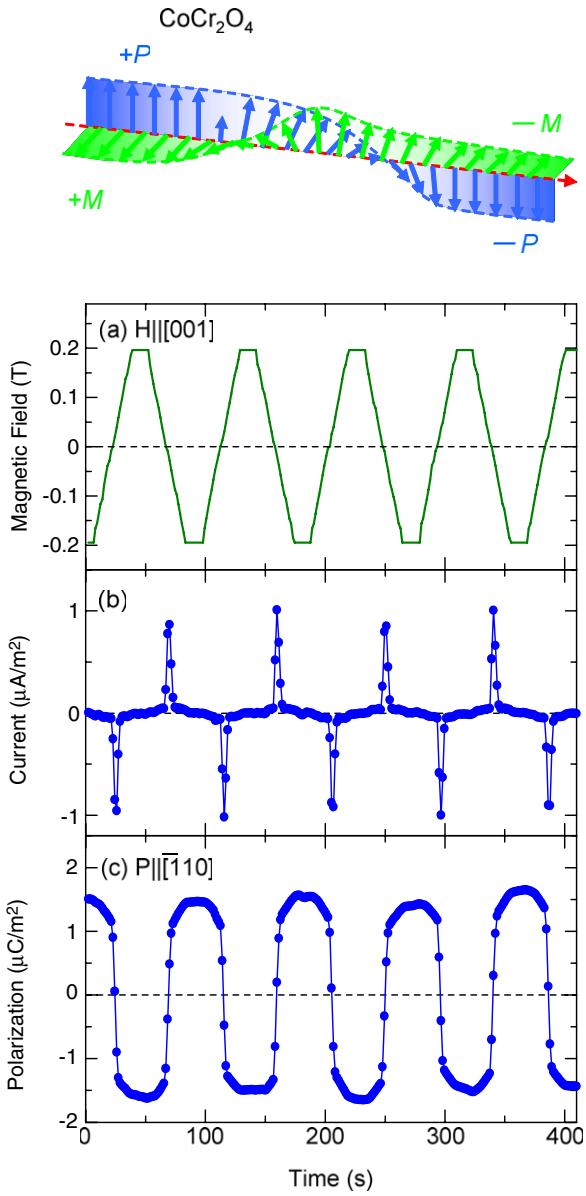

Figure 8. The synchronized reversal of the polarization ($P \parallel y$, closed circles) at 18 K with changes of the external magnetic field ($H \parallel z$) which periodically reverse the magnetization direction ($M \parallel z$); the time profiles of (a) magnetic field, (b) polarization current and (c) polarization. The upper panel depicts the plausible clamping process of the ferromagnetic and polarization domain walls. Cited from [9].

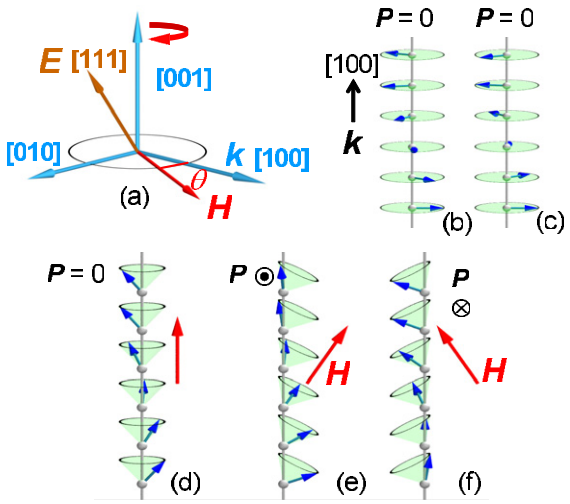

Figure 9. (a) The diagram of the experimental set-up. The magnetic field (H) is rotated in the (001) plane. The electric polarization (P) is measured along the [111] axis. (b) Clockwise and (c) counterclockwise proper screw structure with the propagation vector (k) parallel to the [100]. (d) Proper, and ((e) and (f)) tilted conical spin structures under the external magnetic field. The tilted conical structures ((e) and (f)) produce the ferroelectric polarization.

almost perfectly maintained during the magnetic-field-induced reversal of the magnetization and the polarization. In other words, the ferromagnetic and ferroelectric domain walls are anticipated to be always clamped: the magnetic domain wall, e.g. of the Bloch type, may sustain the similar spin spiral habit and hence the direction of the P may also rotate, while keeping the orthogonal relation with M, as schematically depicted in the upper panel of figure 8.

With these characteristics of the transverse conical spin ferroelectrics, we may further explore new magnetic ferroelectrics in a more broad family of helimagnets: the most ubiquitous form of helimagnets is proper screw type (figures 9(b) and (c)), in which the modulation vector k is perpendicular to the spin spiral plane. According to the spin-current model as expressed by equation (1), however, this form alone cannot produce ferroelectricity, nor even the longitudinal conical form (figure 9(d)). Nevertheless, this class of compounds, most typically $ZnCr_2Se_4$ [32, 33], have been known to show the linear ME effect under $H(\perp k)$ in accord with the group theory's prediction. From the contemporary viewpoint, this feature can be interpreted as the generation of P via the spin-current mechanism in the form of the conical spin structure with the cone axis slanted from the k direction; the summation of local polarization according to equation (1) should result in the macroscopic P whose direction is perpendicular to both the cone axis (or H) and k, as schematically shown in figures 9(e) and (f).

$ZnCr_2Se_4$ forms a cubic spinel structure. Below 20 K [34], spins of Cr^{3+} ions on the B site show a proper screw structure, either clockwise (figure 9(b)) or counterclockwise (figure 9(c)), with the k parallel to [100] [35] and the screw axis aligned along the k due to the easy-plane anisotropy. Under the H applied parallel to the [100] direction, spin forms the longitudinal conical screw as described in figure 9(d). When H is not parallel to the k, the cone is tilted and P is anticipated to be produced in terms of the spin-current model; $P \perp k$ and $P \perp H$ (figures 9(e) and (f)). Figure 9(a) shows the experimental configuration for the P measurement. The rotation angle θ is defined as the angle between [100] and the H direction within the (001) plane. In this configuration, the P which satisfies the relation equation (1) should always appear along the [001] direction. Prior to the measurement of P (or displacement current), the helicity of the spin screw was fixed by the ME cooling procedure.

Figure 10(a) shows the magnetization (M) curves for $H \parallel$ [100] and [210], corresponding respectively to the cases shown

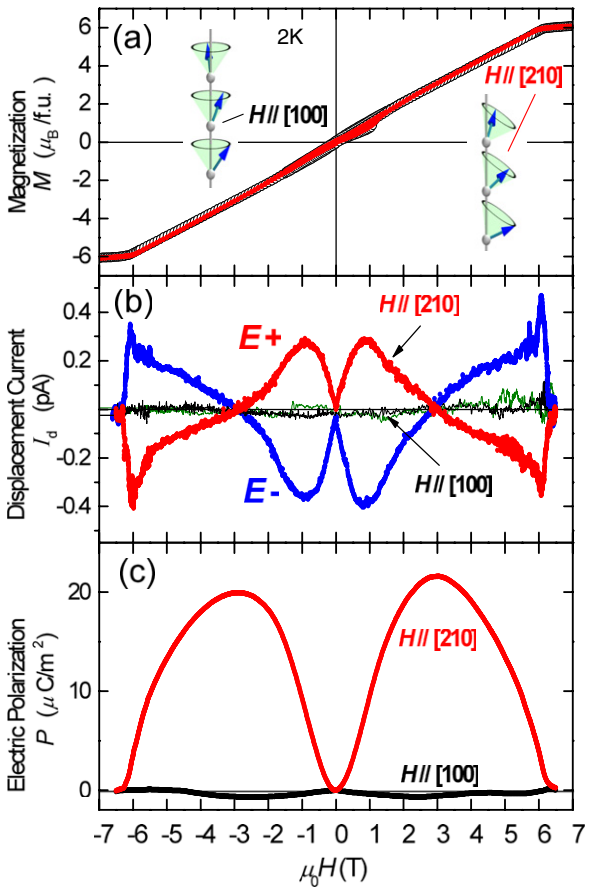

Figure 10. The H dependence of (a) magnetization M, (b) displacement current I_d and (c) electric polarization P of $ZnCr_2Se_4$ under $H \parallel [210]$ and [100] at 2 K. In (b), the I_d taken after the magnetoelectric cooling under positive and negative electric field is indicated as E_+ and E_-, respectively. Cited from [27].

in figures 9(d) and (e) [27]. The M, nearly isotropic except for the low-H region below 2 T, increases linearly with H and is saturated at around 6.3 T, viewed as the transition from the conical to ferromagnetic state, in accord with the result in the literature [36]. We show the H dependence of the displacement current I_d and the derived P in figures 10(b) and (c). When H is applied parallel to the [100] direction, I_d is almost zero and thus P is not observed. For $H \parallel [210]$, on the other hand, the I_d increases with increasing H, shows a maximum at 1 T, and above 1 T decreases with H toward a sign change at 3 T. Around the transition from the helimagnetic to ferromagnetic state, the I_d shows a sharp negative peak, and then becomes zero. As shown in figure 10(b), the sign of I_d is not changed by the inversion of H, but is reversed when the ME cooling is performed using the electric field (E_-) along the opposite direction. The P increases up to around 3 T, and then decreases toward zero at the helical–ferromagnetic transition field. According to the spin-current model [17], the P in the low-H region is governed by the tilting process of the helical plane, while the change of the spin structure in the high-H region is governed by the closing cone angle of the conical spin structure.

Keeping such H-induced ferroelectricity in mind, we discuss the results under rotating H or with changing θ between H and [100] within the (001) plane (see figure 9(a)). In figure 11, we show the θ dependence of P at relatively low H values, where the screw k direction is not changed [27]. (Concerning the higher-H behaviors, that include the k-flop process accompanying the domain-wall dynamics, see the original report by Murakawa and coworkers [27].) When the cone axis of the conical spin structure is parallel to H as shown in the upper panel of figure 11(b), the P is expected to be proportional to $\sin\theta$ (a solid line in the figure). The case of $H = 1.3$ T approximately corresponds to this situation, although the P is observed to show a cusp around 90°. The latter feature is perhaps because the discrepancy angle between the actual cone axis and H direction is large in this field region due to the magnetic anisotropy. At $H = 1.0$ T (figure 11(a)), by contrast, because of the smaller gain of Zeeman energy, the conical axis cannot be perpendicular (parallel) to k (H around $\theta = 90°$). Thus, the original proper screw-like structure is revived for such a low field ($H \sim 1.0$ T) applied perpendicular to k, as shown in the upper panel of figure 11(a). This is the origin of the steep decrease in P around $\theta = 90°$. Judging from the slope of the θ dependence of P, the sign of the spin helicity around $\theta = 180°$ must be opposite to the case of $H = 1.3$ T. Thus, with variation of the H magnitude relative to the magnetic anisotropy, the 180° rotation of H gives rise to the opposite spin helicity (or screw sense).

It is worth noting here that the similar magnetic field control of the P vector with relatively low magnetic field will be possible for a broad family of helimagnets. As one such example, the directional-H control of the ferroelectric polarization through the flexible control of the conical spin axis has also been demonstrated for one of the Y-type ferrites with the composition of $Ba_2Mg_2Fe_{12}O_{22}$ [37]. Reflecting the conical spin structure with the k vector along the specific crystallographic axis (c axis), the rotation of H to any direction off the c axis can produce the ferroelectric polarization along the direction perpendicular to both the k vector and H. The ferroelectric feature can be induced by a low magnetic field as small as 30 mT.

5. Toward electric control of magnetism

The multiferroic state of magnetic origin may in most cases compete with another ME phase, say a paraelectric–antiferromagnetic phase. In the phase-competing region, therefore, the application of magnetic (or electric) field may induce a phase transition between those ME phases, resulting in the magnetic (or electric) control of the ME phases and hence the P (or M). In fact, this is the microscopic origin of the magnetic P control as observed for the spiral spin ferroelectrics. The critical tuning of the ME phase competition may realize the colossal ME phenomena, such as the electric field induction of the ferromagnetic phase, i.e. the function of quantum electromagnets.

An even more remarkable characteristic expected for the multiferroics is the electric reversal of the M vector. The multiferroics of all-spin origin may show the clamping of the ferromagnetic and ferroelectric domain walls, which fixes the relative direction of M and spin helicity (or equivalently P)

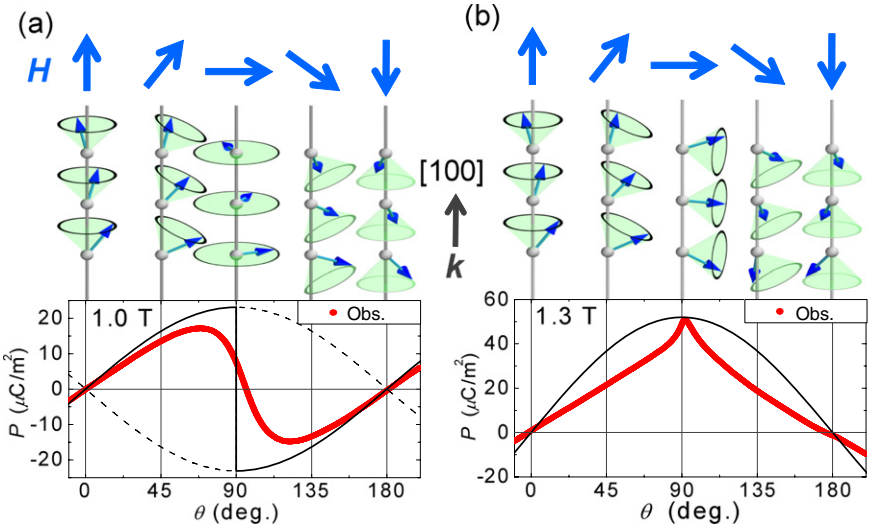

Figure 11. The H rotation angle (θ) dependence of the polarization at (a) 1.0 and (b) 1.3 T. The upper panels illustrate the relation between spin structure and P under rotating H. The upper panels of (a) and (b) illustrate the screw or conical spin structures. The lower panels show the comparison between the observed and calculated P at respective H. Cited from [27].

across the domain wall. The clamping of the ME domain walls is clearly manifested by the magnetic field control of the P direction for $CoCr_2O_4$ [9] and $ZnCr_2Se_4$ [27] with transverse conical spin structure, as partly described in the preceding section. As the inverse effect, such multiferroic conical magnets are expected to show the electric field reversal of the M vector. This may find application in future low energy dissipation electronic devices.

Acknowledgments

The authors thank Y Yamasaki and H Murakawa for their help in preparing the manuscript. This work was in part supported by Grants-In-Aid for Scientific Research from the MEXT, Japan.

References

[1] Schmid H 1994 *Ferroelectrics* **162** 317
[2] Hill N A 2000 *J. Phys. Chem.* B **104** 6694
[3] Smolenskii G A and Chupis I E 1982 *Usp. Fiz. Nauk* **137** 415–48
Smolenskii G A and Chupis I E 1982 *Sov. Phys.—Usp.* **25** 475–93 (Engl. Transl.)
[4] O'Dell T H 1970 *The Electrodynamics of Magneto-Electric Media* (Amsterdam: North-Holland)
[5] Schmid H 2003 Magnetoelectric effects in insulating magnetic materials *Introduction to Complex Mediums for Optics and Electromagnetics* ed W S Weiglhoger and A Lakhtakia (Bellingham, WA: SPIE Press) pp 167–95
[6] Kimura T, Goto T, Shintani H, Ishizaka K, Arima T and Tokura Y 2003 *Nature* **426** 55–8
[7] Goto T, Kimura T, Lawes G, Ramirez A P and Tokura Y 2004 *Phys. Rev. Lett.* **92** 257201
[8] Lawes G *et al* 2005 *Phys. Rev. Lett.* **95** 087205
[9] Yamasaki Y, Miyasaka S, Kaneko Y, He J P, Arima T and Tokura Y 2006 *Phys. Rev. Lett.* **96** 207204
[10] Saito K and Kohn K 1995 *J. Phys.: Condens. Matter* **7** 2855–63
[11] Hur N, Park S, Sharma P A, Ahn J S, Guha S and Cheong S W 2004 *Nature* **429** 392–5
[12] Kimura T, Lawes G, Goto T, Tokura Y and Ramirez A P 2005 *Phys. Rev.* B **71** 224425
[13] Quezel S, Tcheou F, Rossat-Mignod J, Quezel G and Roudaut E 1977 *Physica* B **86–88** 916–8
[14] Kajimoto K, Yoshizawa H, Shintani H, Kimura T and Tokura Y 2004 *Phys. Rev.* B **70** 012401
[15] Kenzelmann M *et al* 2005 *Phys. Rev. Lett.* **95** 087206
[16] Arima T, Tokunaga A, Goto T, Kimura H, Noda Y and Tokura Y 2006 *Phys. Rev. Lett.* **96** 097202
[17] Katsura H, Nagaosa N and Balatsky A V 2005 *Phys. Rev. Lett.* **95** 057205
[18] Sergienko I A and Dagotto E 2006 *Phys. Rev.* B **73** 094434
[19] Mostovoy M 2006 *Phys. Rev. Lett.* **96** 067601
[20] Yamasaki Y, Sagayama T, Goto T, Matsuura M, Hirota K, Arima T and Tokura Y 2007 *Phys. Rev. Lett.* **98** 147204
[21] Taniguchi K, Abe N, Takenobu T, Iwasa Y and Arima T 2006 *Phys. Rev. Lett.* **97** 097203
[22] Park S, Choi Y J, Zhang C L and Cheong S-W 2007 *Phys. Rev. Lett.* **98** 057601
[23] Naito Y, Sato K, Yasui Y, Kobayashi Y, Kobayashi Y and Sato M 2007 *J. Phys. Soc. Japan* **76** 023708
[24] Kimura T, Sekio Y, Nakamura H, Siegrist T and Ramirez A P 2008 *Nat. Mater.* **7** 291–4
[25] Kimura T, Lashley J C and Ramirez A P 2006 *Phys. Rev.* B **73** 220401(R)
[26] Arima T 2007 *J. Phys. Soc. Japan* **76** 073702
[27] Murakawa H, Onose Y, Ohgushi K, Ishiwata S and Tokura Y 2008 *J. Phys. Soc. Japan* **77** 043709
[28] Menyuk N, Dwight K and Wold A 1964 *J. Physique* **25** 528–36
[29] Lyons D H, Kaplan T A, Dwight K and Menyuk N 1962 *Phys. Rev.* **126** 540–55
[30] Tomiyasu K, Fukunaga J and Suzuki H 2004 *Phys. Rev.* B **70** 214434
[31] Funahashi S, Morii Y and Child H R 1987 *J. Appl. Phys.* **61** 4114–6
[32] Siratori K and Kita E 1980 *J. Phys. Soc. Japan* **48** 1443–8
[33] Siratori K, Akimitsu J, Kita E and Nishi M 1980 *J. Phys. Soc. Japan* **48** 1111–4
[34] Menyuk N, Dwight K, Arnott R J and Wold A 1966 *J. Appl. Phys.* **37** 1387–8
[35] Plumier R 1966 *J. Physique* **27** 213
[36] Hemberger J, Krug von Nidda H A, Tsurkan V and Loidl A 2007 *Phys. Rev. Lett.* **98** 147203
[37] Ishiwata S, Taguchi Y, Murakawa H, Onose Y and Tokura Y 2008 *Science* **319** 1643–6